Broadband Radio Interferometer Utilizing a Sequential Triggering Technique for Locating Fast-moving Electromagnetic Sources Emitted from Lightning

R. Mardiana, T. Ushio, Y. Ota, M. Murakami, Z. Kawasaki, K. Matsuura
Department of Electrical Engineering, Osaka University, JAPAN

Abstract

A broadband radio interferometer to investigate the location of fast-moving electromagnetic sources emitted from lightning discharges has been designed and tested. A sequential triggering technique was applied to the system for recording the data of electromagnetic pulses, once the electromagnetic pulse is detected and its amplitude exceeds a threshold level, the triggering circuit is turned on to record the waveform for 1 microsecond and ready to acquire another pulse afterwards. This technique can record 2000 electromagnetic pulses maximum. We have implemented our system to locate and retrace fast-moving electromagnetic sources emitted from lightning discharges during a field experiment in Australia in December 1997. We succeeded to reconstruct a cloud to ground lightning discharge and displayed it in two dimensions and in time sequences.

1. Introduction

Electromagnetic radiation from lightning flashes is characterized by broadband spectrum from a few kHz through several GHz. A lightning flash typically has an interval in the range of hundred milliseconds, and during the occurrence of a lightning flash broadband EM radiation are emitted continuously [e.g. Le Boulch et al., 1990]. Because of lightning spectrum has very large bandwidth, a high digitization rate is needed to record its broadband signals, but since the memory of digitizer is limited, the entire radiation from a lightning flash cannot be recorded. Also, it does not practice if the digitizer has to record the signals having undetected broadband pulses during a lightning flash. To overcome above reason, a sequential triggering technique was proposed where the instrumentation initiate to acquire data only if a lightning flash emits broadband pulses exceeding a threshold level.

Shao et al. [1] have illustrated the basic principle of a broadband interferometer and used this technique in one spatial dimension. Ushio et al. [2] reported more clearly the use of broadband interferometer for locating fast-moving electromagnetic sources with 500 MHz sampling rate and mapping the sequence of lightning discharge processes in two dimension.

In this paper we give the detail principle of our broadband interferometer, experimental setup along with the sequential triggering technique and reports one of the experimental results.

2. Detail of a broadband interferometer

2.1 Basic principle

The basic idea of this interferometer technique is to estimate the phase differences at various frequency components of Fourier spectra between a pair of broadband antenna sensors. The simplest radio interferometer consists of two separated receiving antenna sensors. Consider two broadband antenna sensors separated horizontally above the ground by distance d, as shown in figure 1, the broadband signal which is originated from a common source impinging on antenna 1 is $r_k(t)$ and on antenna 2 is $r_l(t)$. Assuming a total record length is T, then deriving the signals in frequency domain [3] using Fourier transformation, we have equations

$$R_k(f) = \int_0^T r_k(t) e^{-j2\pi ft} dt$$

$$R_l(f) = \int_0^T r_l(t) e^{-j2\pi ft} dt \qquad (1)$$

The cross correlation between both signals is related to the cross power spectral density function by the well-known relationship

$$G_{kl}(f) = R_k^*(f).R_l(f) \qquad (2)$$

where * denotes the complex conjugate. The $G_{kl}(f)$ will generally be a complex number such that

0-7803-5276-9/99/$10.00 © 1999 IEEE

$$G_{kl}(f) = G_{Re}(f) - jG_{Im}(f) = |G_{kl}(f)|\, e^{-j\varnothing(f)} \quad (3)$$

where

$$|G_{kl}(f)| = [G_{Re}(f)^2 + G_{Im}(f)^2]^{1/2}$$

$$\varnothing(f) = atan[G_{Im}(f)/G_{Re}(f)] \quad (4)$$

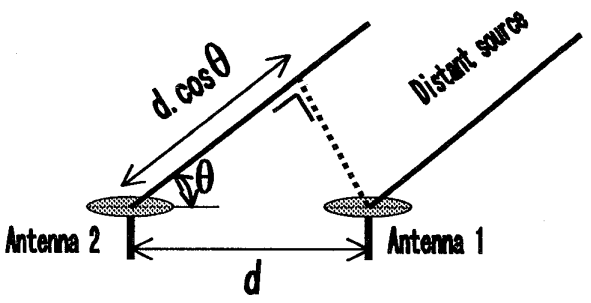

Figure 1. Two broadband antennas separated horizontally.

The term $\varnothing(f)$ of equation 4 corresponds to the phase difference of signal $r_k(t)$ and $r_l(t)$ for each frequency component. Hence, time delay τ between those signals appears in the cross energy spectral as a phase function

$$\varnothing(f) = 2\pi f\tau. \quad (5)$$

For the source is sufficiently distant to be approximated by a plane wave at the receiver locations, the time delay or phase difference can be interpreted as an angle of incidence $\theta(f)$ for the received signal given by

$$\theta(f) = acos[c\tau/d] = acos[c\varnothing(f)/(2\pi fd)] \quad (6)$$

where c and d are the EM propagation speed and the separation distance between the receivers, respectively. The mean value of incident angle can be taken by averaging the θ of each frequency components. To illustrate the above relation (Equation 6) between the incident angle θ and the phase difference $\varnothing(f)$, a computer simulation has been made. The two antennas are assumed to be separated horizontally by 10 m with the corresponding two antennas are identical. Figure 2 shows $\varnothing(f)$ as a function of frequency for several different θ values. The frequency is limited to a range of 0 to 250 MHz; it is shown that the phase difference $\varnothing(f)$ increases proportionally with increasing the frequency.

In practice, the continuous signal will be digitized into digital data. For digital data processing with a recording time T and a sampling interval Δt there will be $T/\Delta t = N$ data points, thus, the discrete frequencies will be separated by $\Delta f = 1/T = 1/(\Delta t.N)$ and the upper frequency limit of the analysis is $f_c = 1/(2\Delta t)$. Hence, for the equations 1 to 6 the frequency increment will be Δf with the highest frequency f_c.

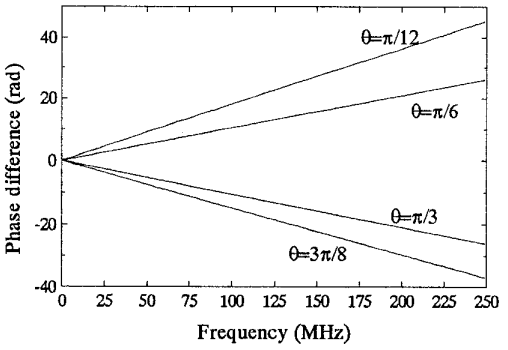

Figure 2. Phase difference as a function of frequency for some different incident angles.

2.2 Crossed base line geometry

Using two-antenna sensors as the first base line, we only can image one-dimensional localization. To provide two-dimensional system, a second base line perpendicular to the first base line is added to determine actual angles of arrival (azimuth and elevation) as described by Hayenga [4]. The second base line can consist of two antennas and one of which as a common antenna with the first base line. Figure 3 shows the basic geometry of a perpendicular crossed baseline interferometer.

For simplicity, consider a source in the northeast quadrant. Each base line provides a direction cosine between the source and the respective base line. Let θ_1 and θ_2 are the incident angles of the source for the first base line and the second base line, respectively. The azimuth (α), elevation (β), and θ_1 form one right spherical triangle, while $(90-\alpha)$, β, and θ_2 form another. In this geometry $\alpha = 0^o$ implies due east and $\alpha = 90^o$ implies due north. Using the relations

$$cos\,(\theta_1) = cos\,(\alpha)\, cos\,(\beta) \quad (7)$$

and

$$cos\,(\theta_2) = cos\,(90-\alpha)\, cos\,(\beta)$$

$$= sin\,(\alpha)\, cos\,(\beta) \quad (8)$$

and by dividing equation 8 with equation 7, with the constrain $\theta_1 \neq 90^o$ and $\beta \neq 90^o$, we obtain

$$\tan(\alpha) = \cos(\theta_2) / \cos(\theta_1)$$

or

$$\alpha = \operatorname{atan}[\cos(\theta_2)/\cos(\theta_1)] \quad (9)$$

Finally, we determine β, as

$$\beta = \operatorname{acos}[\cos(\theta_1)/\cos(\alpha)] \quad (10)$$

or equivalent with

$$\beta = \operatorname{acos}[\cos(\theta_2)/\sin(\alpha)].$$

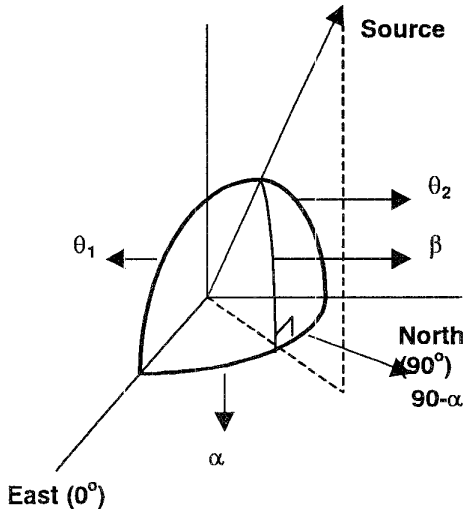

Figure 3. The east-west as the first base line measures the incident angle θ_1, and north-south as the second base line measures the incident angle θ_2. The azimuth (α) and elevation (β) can be determined from those incident angles.

3. Experimental Setup

An experiment to locate fast-moving electromagnetic sources emitted from lightning discharges was conducted in Darwin, Australia in December 1997. The system employed three broadband flat plane antennas, which were separated horizontally with the baseline's length about 10 meters and aligned at three apexes of a square. The antennas were connected to a digitizer by coaxial cables and high-pass filter (>25 MHz). The broadband lightning *dE/dt* signals were digitized at 500 MHz sampling rate using a digitizer which was controlled by a Personal Computer (PC) through IEEE-488 port. Because of such high digitization rate, the entire radiation from a lightning flash cannot be recorded continuously. For example, in order to record one second long stream, 500 Mwords memory per-channel of digitizer is required, which does

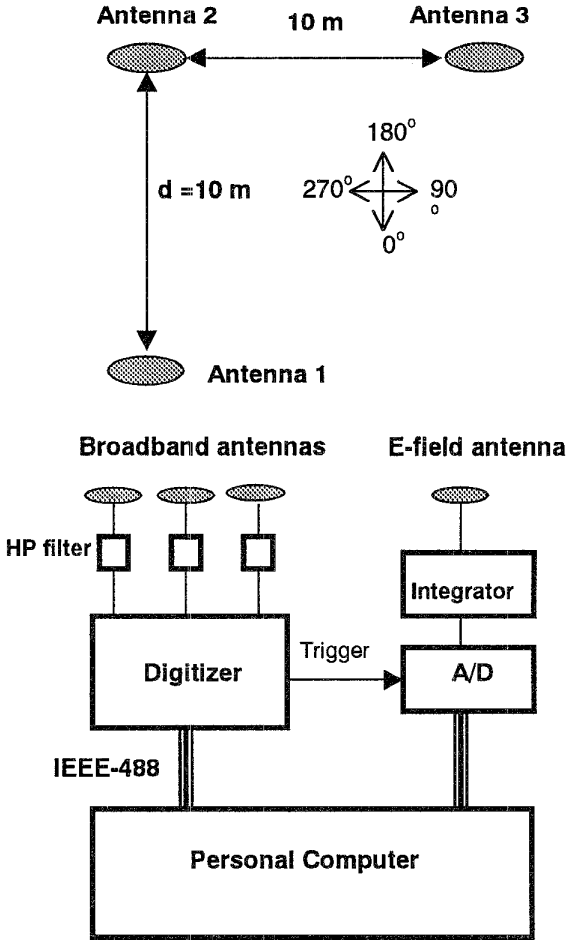

Figure 4. A broadband measurement system. (a) antenna configuration, antenna 1 and 2 as the first baseline and antenna 2 and 3 as the second baseline. (b) electronic instrumentation.

not practice. To overcome this difficulty, we applied a sequential triggering technique for each electromagnetic pulse. We divided the whole memory of digitizer into 2000 segments, and each segment can record one broadband electromagnetic pulse for T = 1 microsecond or N = 502 data points. Once the electromagnetic pulse from lightning flash is detected and its amplitude exceeds a threshold level, the triggering circuit is turned on to record a waveform and save it as one segment. The minimum time between two consecutive radiation sources is about 70 μs due to instrumentally dead time. With this technique, we can record maximum two thousand broadband electromagnetic pulses with the length of

recording time is 1 second. The system was operated to record radiation sources from 25 to the upper limit frequency f_c = 250 MHz.

The processing of the broadband signals is similar to that described by Ushio et al. [2] as follows: (1) a discrete Fourier transform is applied to extract the phase difference of incident electromagnetic pulses at two antennas; (2) the mean incident angles respective to the antennas base lines are computed; (3) finally, the azimuth and elevation angles of radiation sources are resolved.

A fast antenna having a time constant of 100 μs and sampling rate 1 MHz was also equipped to measure electrostatic field changes (E) and connected to the same PC. The synchronization between the fast antenna and the broadband antenna system is within 1 microsecond. Figure 4 shows the broadband measurement system illustrating the broadband antenna configuration and the electronic instrumentation including the electrostatic field measurement. This station was capable of recording dE/dt and E radiation from multiple impulsive events (return stroke, leader steps, cloud discharges, etc) within individual lightning flashes, with sub-microsecond time resolution, and of placing these events in the context of the flash as a whole.

4. Results

As a case study, we will pay particular attention to a data from a cloud to ground lightning flash, which was detected during the campaign. This flash lasted about 400 ms from the beginning of broadband pulses and 347 segments were successfully recorded. Figure 5(a) shows the first ten segments of broadband pulses from antenna 1 and figure 5(b) shows the expanded scale of the broadband pulse from the fifth segment for all antennas, it is clearly seen the difference of arrival-time delay among signals. To simplify the next explanation of broadband interferometer processing, we will focus on the signal from this fifth segment only. Using a discrete Fourier transform, the amplitude and phase of this signal as a function of frequency can be shown in figure 6 for all antennas. These phases seem to have random values for all frequencies, but the phase difference have a tendency to form a constant slope as shown in figure 7(a) for each baseline, and they are consistent with equation 5 or the graphic on figure 2. No phase difference values from frequency range of 0 to 25 MHz is provided because of filtering. To find the incident angle of radiation source for each frequency component, the equation 6 is applied to those values of phase differences, and the result for each baseline can be seen in figure 7(b). By averaging these incident angles to estimate a mean value, and by using equation 9 and equation 10, finally, the angular position or azimuth and elevation of this radiation source can be determined.

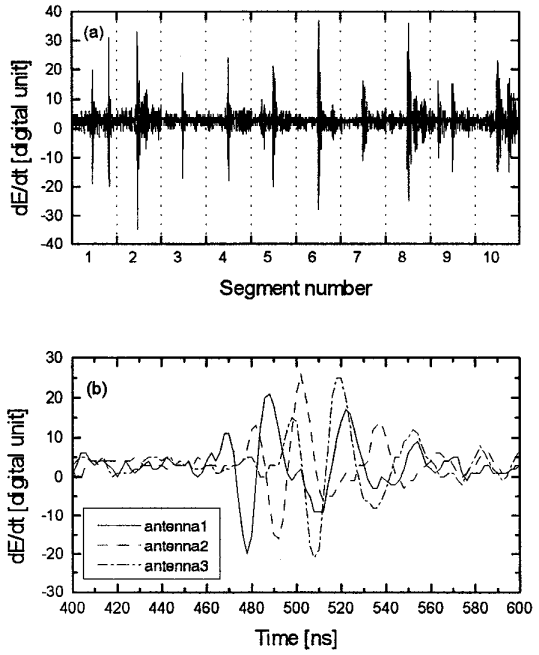

Figure 5. Broadband signals. (a) The first ten segments of broadband signal received by antenna 1. (b) Expanded scale of the fifth segment to show the arrival time delay of each broadband signal impinging on the antennas.

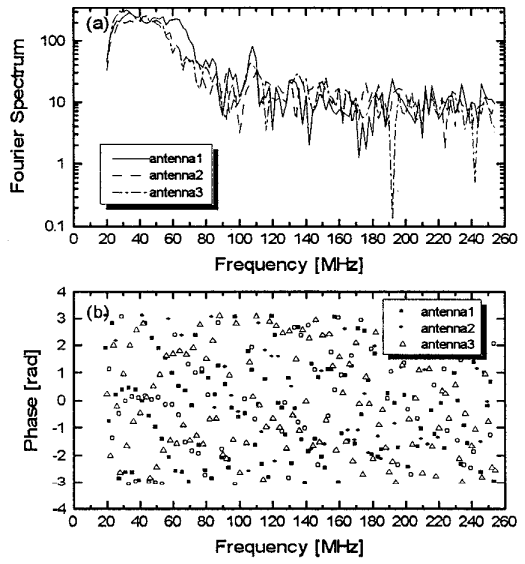

Figure 6. Fourier spectrum of the fifth segment for each antenna. (a) Amplitude. (b). Phase.

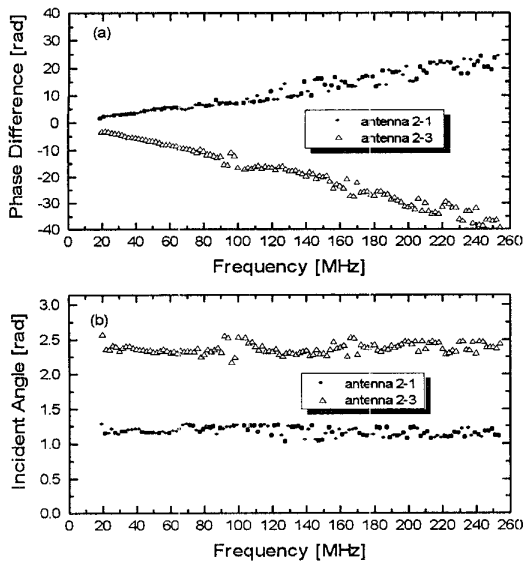

Figure 7. Phase differences and incident angles of the fifth segment. (a) Phase difference has a tendency to form a constant slope with increasing frequencies. (b). Incident angle for each frequency. The mean value of these incident angles is used to determine the angular position.

All successful segments can be mapped in angular-time format and azimuth-elevation format. Figure 8 displays the activity of the flash in both formats, a dot represents an angular position from a segment, and an electric field waveform together with labeling A, B, and C are also provided to simplify explanation to this lightning event. During A1 period, the flash began with cloud discharge activity with no significant changed in electric field. Strong broadband radiation was detected during the first leader progression moving downward in event A2. In this instance the leader required about 12 ms to reach ground and the electric field change was negative indicating that negative charge was transported toward the observation site, or equivalently, that positive charge was transported away the site. The activity culminated with an abrupt electric field change just beyond the end of A2, caused by a return stroke. During event B1, the radiation was emitted rarely and because of the angular position of this radiation was above ground level, this activity could be inside cloud discharges. The second leader progression to ground appeared during event B2 along with strong broadband radiation, since the leader channel has the same angular position with A2 event, so the second leader channel followed the path taken by the first leader. The radiation ceased at the beginning of return stroke, whose electric field changed abruptly. This leader completed its extension within 15-18 ms. The last activity of this flash, similar to

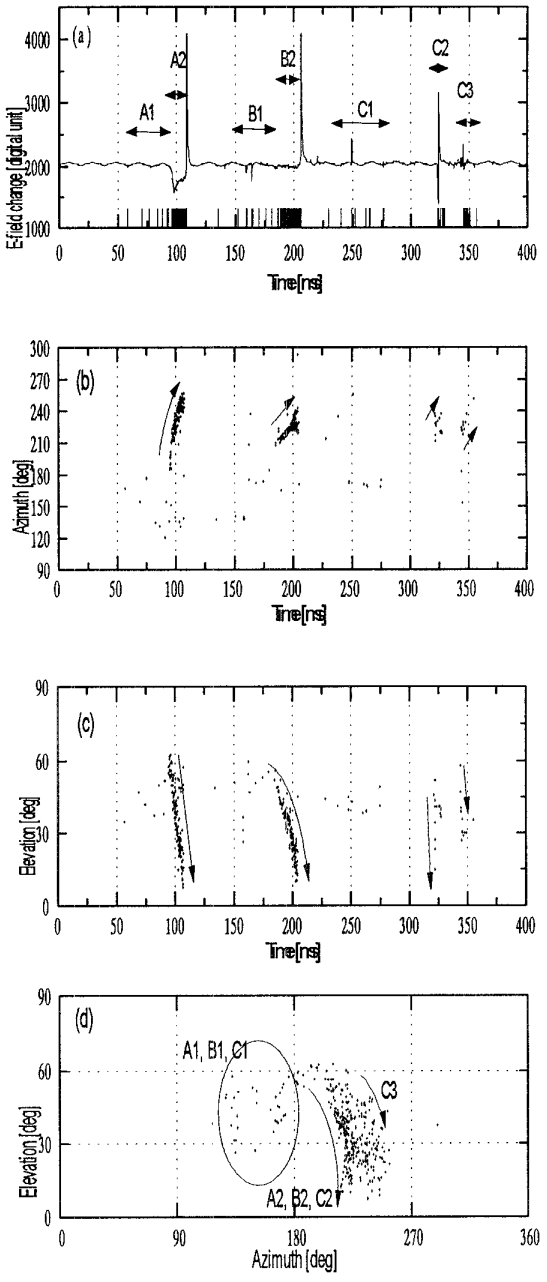

Figure 8. Activity of a cloud to ground flash. (a) Electric field change, the series of time tags indicated by thin vertical lines at the time axis shows the time when the broadband signals were received. (b) Azimuth position of radiation sources in time sequences. A dot represents an angular position from a segment. (c) Elevation position of radiation sources in time sequences. Three leaders propagating downward the ground can be identified. (d) Angular position. All leader channels nearly have the same angular position.

event B1, we recorded some isolated radiation during event C1 where the position was inside the cloud. The fast field change during the very short period of within 2-4 ms in event C2 shows the third leader progression followed by a return stroke. The path of this leader channel was also the same with the previous leaders in event A2 and B2. Such discharges propagating downward inside the clouds labeled C3 remained occur after several milliseconds from the last return stroke.

5. Conclusions

A broadband interferometer technique for locating fast-moving electromagnetic sources emitted from lightning has been introduced and demonstrated. The basic principle of this technique is to extract the phase difference at various frequency components of Fourier spectra between a pair of broadband antenna sensors, and thereafter the incident angle of radiation sources can be determined. A high digitization rate was used to overcome the large lightning bandwidth and a sequential triggering technique was used to overcome the limitation of digitizer memory. Our memory of digitizer was divided into 2000 segments maximum and each segment can record one broadband electromagnetic pulse for 1 microsecond and the maximum recording time was 1 second. One segment corresponds to one angular position of lightning radiation source.

We analyzed a cloud to ground flash having several leader progression as a case study. From this flash, 347 segments had successfully been recorded within 400 ms. The lightning discharge processes were preceded by cloud discharges in the early stage of first and subsequent leaders. Strong electromagnetic pulses were detected along with the leader progression, and then an abrupt electric field change following a return stroke occurred just after each leader reached the ground. The first, second and third leaders have duration about 12 ms, 15-18 ms and 2-4 ms, respectively, and the interval between the return strokes was about 100 ms and 140 ms. All leader channels have the same angular position, indicating that subsequent leaders followed the channel path taken by the first leader to ground.

References

[1]. Shao, X.M., D.N Holden and P.R. Krehbiel, "Broadband radio interferometry for lightning observation", Geophys. Res. Lett., 23, 1917-1920, 1996.

[2]. Ushio, T., Z. Kawasaki, Y. Ohta, K. Matsuura, T. Watanabe and X. Liu, "Manufacture of broadband interferometer and observation of lightning discharges in China", Scientific Meeting: Institute of Electrical Engineers of Japan, ED-97-118~149,155-160,1997 (*in Japanese*).

[3]. Piersol, A.G., "Time Delay Estimation using Phase Data", IEEE Transc. ASAP-29, No.3, June 1981.

[4]. Hayenga, C. O., and J. W. Warwick, "Two-dimensional interferometric positions of VHF lightning sources", J. Geophys. Res., 86, 7451-7462, 1981.

[5]. Mardiana, R., Y. Ohta, M. Murakami, T. Ushio, Z. Kawasaki, K. Matsuura, "A Broadband radio Interferometer for Observing Lightning Discharge Processes", J. Atmosph. Electricity, 18, 111-117, 1998.

[6]. Proctor, D. E, "A hyperbolic System for Obtaining VHF Radio Pictures of Lightning", J. Geophys. Res., 76, 1478-1489, 1971.

[7]. Rhodes, C.T., X.M. Shao, P.R. Krehbiel, R.J. Thomas and C.O. Hayenga, "Observation of lightning phenomena using VHF radio interferometry", J. Geophys. Res., 99, 13059-13082, 1994.